1. Assessment of shoreline change

An analysis of the spatial and temporal changes in the Adriatic littoral zone between Barletta and Manfredonia was carried out by the digital extraction of the shorelines from available aerial photos, orthophotos, satellite images, and LiDAR data. They were collected for a medium-term analysis and integrated with TLS data acquired at different times (hours/days). The multitemporal shorelines were digitalized in ArcGIS for every year. Digital Shoreline Analysis System (DSAS) tools were also used in order to obtain the shoreline 1869 to 2019 changes (**Table S1**). During the processing, uncertainty about the position of the shoreline was defined. The following factors were considered:

Line drawing of the operator on the swash zone with an error range of ±3 m

Weather conditions (tidal range, atmospheric pressure, temperature, sea level, wind) at the time of image acquisition with an error range of ±0.4 m

Instrumental accuracy with an error range of 0.31–0.5 m

For each time span, the minimum, maximum, weighted average, and error range were evaluated. The choice of the weighted average is related to the density data for a given time range.

Table S1. Dataset used for the assessment of shoreline positions in the different years.

Year of images	Type of data	Accuracy
1869	Topographic map of *Istituto Geografico Militare*	25 m
1909	Topographic map of *Istituto Geografico Militare*	25 m
1954	Topographic map of *Istituto Geografico Militare*	25 m
1988	Aerial photographs	5 m
1997	Aerial photographs	5 m
2006	Aerial photographs	5 m
2009	Terrestrial Laser Scanner	0.05 m
2010	Satellite image World View 2	0.45 m
2013	Aerial photographs	3 m
2019	Aerial photographs	3 m
2020	Satellite image Landsat 8	12 m

Taking into account the sea-level rise records at the Manfredonia AdB station (**Figure S1**), different horizontal displacement rates, in function of the coastal slopes, can be derived. Secondly, geometric horizontal shoreline movements due to sea-level rise were subtracted from the observed shoreline movements in order to obtain effective shoreline change (**Table S2**) and to apply a correct value of horizontal displacement.

The submersion model of Scardino et al. [1] along a sandy coast requires the knowledge of the following parameters: (i) sea-level trend; (ii) VLM rates,; and (iii) shoreline erosion/accretion. The model was implemented mathematically in a Matlab environment by considering the components conditioning both the vertical and horizontal coastal displacements for the sea level and shoreline changes:

$$\Delta z = SL \pm \Delta z_{\text{tide}} \qquad (1)$$

$$\Delta x = v_{\text{LRR}} \times \Delta t \times \cos\beta \qquad (2)$$

$$\Delta y = v_{LRR} \times \Delta t \times \sin\beta \quad (3)$$

where:
Δz—vertical shoreline displacemet (m)
SL—sea level at a given year (m)
Δt—prediction time span (year)
Δz_{tide}—tide amplitude (m)
Δx—easting shoreline displacement (m)
Δy—northing shoreline displacement (m)
v_{LRR}—effective shoreline rate changes (m/year)
β—normal shoreline angle (degrees).

The output provides all the points corresponding to the submersion surfaces at multi-temporal times, predicted up to 2150, and presented in a GIS-layer format with the xyz coordinates in WGS84 UTM zone 33N metric reference.

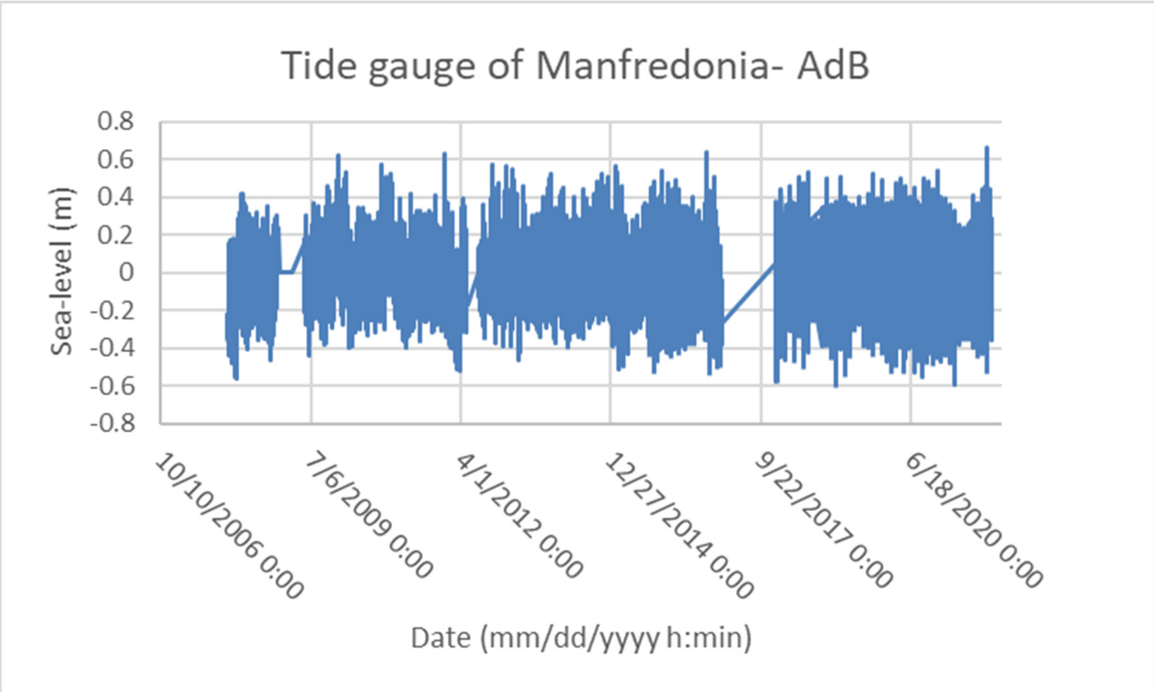

Figure S1. Time series of tidal data recorded at the station of Manfredonia (property of Autorità di Bacino della Puglia); the linear regression is equal to 3.5± 0.2 mm/yr.

Table S2. Shoreline rate changes assessed in the studied areas of Tavoliere delle Puglie (Figure 4 of the main text); A – the six study areas used for the sea-level projections; B – coastal slope; C – rates of shoreline erosion in a steady-state conditions of the coastal zone; D – rates of shoreline erosion assessed through linear regression of the data; E- effective shoreline changes obtained from the difference between D and C columns.

A		**B**	**C**	**D**	**E**
Zone		**Coastal Slope (degree)**	**Rates due to relative sea-level rise(m/yr)**	**Observed rates of shoreline erosion (m/yr)**	**Effective shoreline change (m/yr)**
Area 1	Manfredonia	1.46	0.004 ± 0.002	-0.200 ± 0.06	-0.196 ± 0.06
Area 2	Siponto	0.17	0.021 ± 0.002	-1.100 ± 0.32	-1.079 ± 0.32
Area 3	Ippocampo	0.03	0.117 ± 0.002	-3.100 ± 0.89	-2.983 ± 0.89
Area 4	Zapponeta	0.03	0.117 ± 0.002	-2.850 ± 0.82	-2.733 ± 0.82
Area 5	Torre Pietra	0.04	0.088 ± 0.002	-2.850 ± 0.83	-2.762 ± 0.83

Area 6	Margherita di Savoia	0.14	0.025 ± 0.002	-5.850 ± 1.75	-5.825 ± 1.75

The most relevant shoreline changes have been observed on the coastal plain of Area 3 (**Figure S2**), and Area 6 (**Figure S3**). These two areas were subjected to intensive anthropogenic impact, with building of touristic resorts and coastal defence structures, which determined a negative sedimentary balance. Another important factor that conditioned the sedimentary balance was the decrease on the solid load delivered by Ofanto river in the last decades. This is reflected in a shoreline retreat of about 200 m from 1954 to 2019.

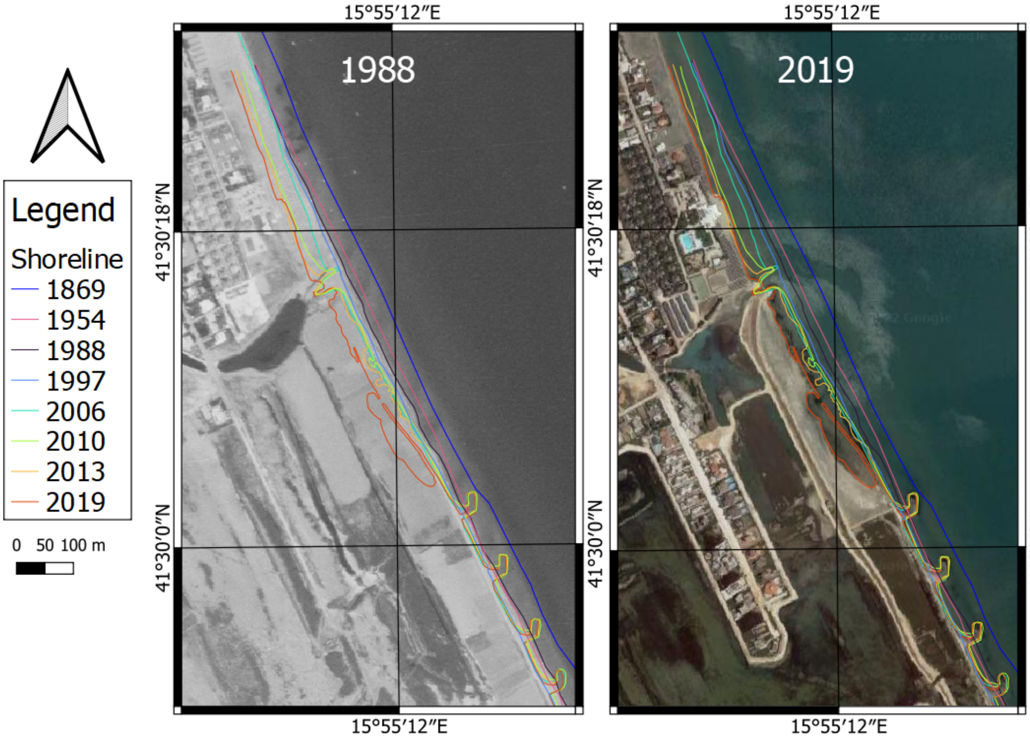

Figure S2. Shoreline erosion in the Ippocampo area as assessed through historical maps, aerial photographs and satellite images. Here, digitized contours of the shoreline in several years are shown superposed to two representative images: an aerial photo acquired in 1988 (left – aerial photograph of Istituto Geografico Militare) and a satellite image acquired in 2019 (right - aerial photograph of Agenzia per Erogazioni in Agricolutra AGEA).

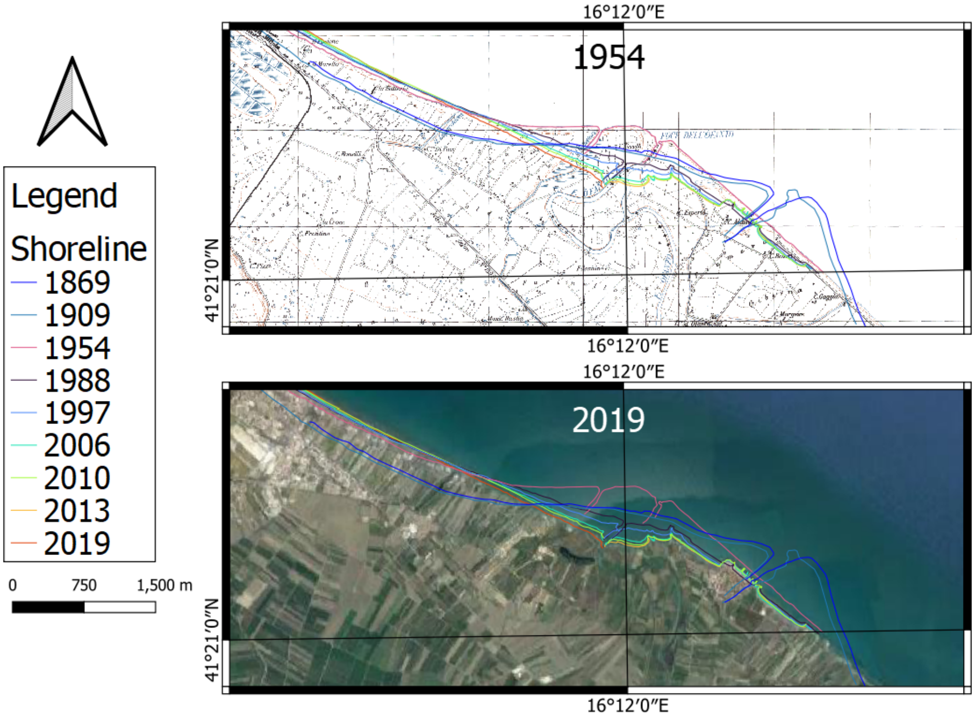

Figure S3. Shoreline erosion in the Margherita di Savoia and Ofanto river mouth as assessed through historical maps, aerial photographs and satellite images. As in Figure S2, shoreline contours are superposed on a historical 1954 map (top – source of Istituto Geografico Militare) and on a satellite image acquired in 2019 (bottom – aerial photograph of Agenzia per Erogazioni in Agricolutra AGEA).

2. XBeach storm modelling

Because the characteristics of storm wave propagation are very different from deep to shallow waters, the modelling process implies the use of different grid resolutions to reproduce wave dynamics at different spatial scales[2,3]. For this reason, the simulation of the storm wave propagation from its source region (offshore) to the coastal area was carried out by nesting grids with varying resolutions in DelftDashboard. The coarser grid was built with 80 × 80 m cells and is located offshore of Gulf of Manfredonia. The finer grid was built with 4 × 4 m cells along the coastal areas. Bathymetric data of Italian Hydrographic Institute were used to interpolate the offshore bathymetry (property of Italian Hydrographic Institute – Italian Royal Navy).

The wave propagation on the finer grid was computed by the XBeach model, to assess the inland flooding. The largest storm event recorded in the Adriatic sea was considered as reference to establish the meteo-marine parameters. XBeach requires the spectra parameters of the waves, which were assessed using a JONSWAP Spectra characterized by significant wave height (Hm0) and peak period (Tp) (**Table S3 and Figure S4**).

Table S3. Spectral parameters of JONSWAP for the assessment of storm impact; Hm0: significant wave height; Tp(s): peak period; mainang: wave direction in nautical degree; water level during the storm event.

Time from start of simulation (s)	Hm0 (m)	Tp (s)	mainang (nautical degree)	gammajsp - Peak enhancement factor	s - Directional spreading coefficient	Water level
3600	0.51	4.1	85	3.3	10	0.25
7200	0.58	2	90	3.3	10	0.48
10800	0.59	3.5	95	3.3	10	0.15

14400	0.52	4	102	3.3	10	0.57
18000	0.6	4.5	102	3.3	10	0.2
86400	1.18	5	103	3.3	10	0.49
172800	2	5.2	103	3.3	10	0.2

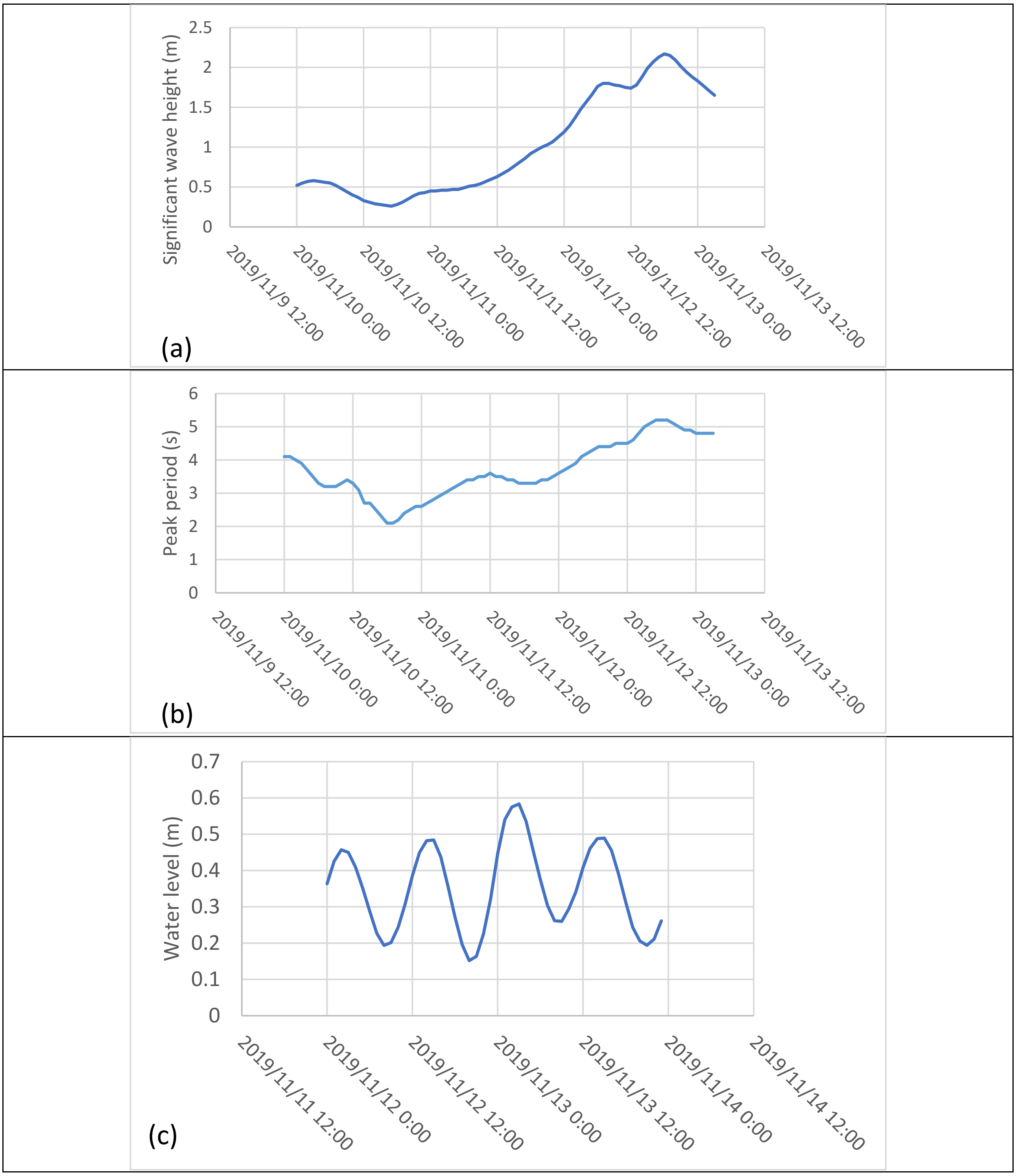

Figure S4. Spectral parameters of JONSWAP; **(a)** time-series of significant wave height Hm0; **(b)** time-series of peak period Tp; **(c)** time-series of water level during the storm event of 11-14 November 2019.

Reference

1. Scardino, G.; Sabatier, F.; Scicchitano, G.; Piscitelli, A.; Milella, M.; Vecchio, A.; Anzidei, M.; Mastronuzzi, G. Sea-Level Rise and Shoreline Changes Along an Open Sandy Coast: Case Study of Gulf of Taranto, Italy. *Water* **2020**, *12*, 1414, doi:10.3390/w12051414.
2. Roelvink, D.; Reniers, A.; van Dongeren, A.; van Thiel de Vries, J.; McCall, R.; Lescinski, J. Modelling Storm Impacts on Beaches, Dunes and Barrier Islands. *Coastal Engineering* **2009**, *56*, 1133–1152, doi:10.1016/j.coastaleng.2009.08.006.
3. Roelvink, D.; Costas, S. Coupling Nearshore and Aeolian Processes: XBeach and Duna Process-Based Models. *Environmental Modelling & Software* **2019**, *115*, 98–112, doi:10.1016/j.envsoft.2019.02.010.
4. Ferrarin, C.; Bajo, M.; Benetazzo, A.; Cavaleri, L.; Chiggiato, J.; Davison, S.; Davolio, S.; Lionello, P.; Orlic, M.; Umgiesser, G. Local and Large-Scale Controls of the Exceptional Venice Floods of November 2019. *Progress in Oceanography* **2021**, *197*, 102628, doi:10.1016/j.pocean.2021.102628.